Calculating Pavement Deflections with Velocity Transducers

R. Clark Graves and Vincent P. Drnevich

Pavement engineers and researchers agree that valuable information can be obtained from surface deflection basin measurements of pavements. Several methods of applying a load to the pavement to cause pavement deflections have been used for many years, including static, vibratory, and impulse types of loadings. Vibratory and impulse loadings typically use velocity transducers to measure the corresponding surface deflections. Methods used to calculate pavement deflections caused by impulse loadings are complex. A good understanding of signal analysis and the theory of vibration is needed to accurately calculate pavement deflections from the transducer outputs. An overview of the various procedures required to accurately calculate these deflections is provided. A three-part study has been conducted: theoretical modeling of the transducer response, laboratory calibration of the transducer response, and comparison of independently determined deflections with those from an impulse loading test, referred to as a falling weight deflectometer.

In the past few years, there has been increasing interest in the long-term monitoring of pavement performance. Nondestructive testing has proven to be a good tool for evaluating the structure of in-service pavements.

Pavement engineers and researchers agree (*1*) that pavement surface deflection basin measurements, nondestructive tests, provide valuable information on the structural condition of pavement systems. Pavement deflections depend on the magnitude and mode of loading (steady state, impulse, or vehicular). The ideal response measurements for structural evaluation are those produced under actual design traffic loads, but these are not practical now (*1*).

Several techniques have been used for nondestructive pavement testing. They are typically divided into three categories: static deflection measurements, steady-state vibration deflection measurements, and impulse deflection measurements.

The steady-state and impulse devices both use velocity transducers to calculate pavement deflections. However, the method of deflection calculation is considerably different for the impulse devices because of the nature of the loading. The steady-state devices operate at a fixed frequency, which is normally in the linear range of the transducers. Therefore, a direct integration of the transducer output provides the pavement deflection.

Impulse testing is generally conducted with a falling weight deflectometer (FWD). A weight is lifted a given height above the pavement and dropped onto a spring-buffer system. The spring-buffer system transfers the load to the pavement over approximately 30 msec. The load applied to the pavement and the vertical motions at various radial distances from the center of the load are measured by using velocity transducers. The load is adjusted by varying the drop height and the weight. The deflections at the radial distances are calculated from the outputs of the velocity transducers.

Impulse-testing devices generate a transient response, which has frequency components that are predominantly between 0 and 100 Hz. Because the response of the velocity transducer is not constant across the entire frequency range, a direct integration of the transducer output does not provide the displacement of the pavement. The response characteristics of the transducer across the entire frequency range are required to calculate accurate pavement deflection time histories.

The goal of this study was to gain a better understanding of the transducers typically used with FWD measurements, to evaluate their accuracy, and to develop a technique for obtaining accurate pavement displacement time histories. A three-phase study was conducted: theoretical modeling of the transducer response, laboratory calibration and validation of the transducer response, and comparison of independently determined deflections with those from an impulse loading test using an FWD (*2*). This research confirms and builds on the information presented by Nazarian and Bush (*3*) for the frequency response function approach.

PHASE 1: THEORETICAL TRANSDUCER RESPONSE

Background

Velocity transducers (geophones) may be modeled as damped single-degree-of-freedom (SDOF) systems. Geophones are typically coil-magnet systems, as shown in Figure 1. A mass having an attached magnetic coil (labeled "conductor" in Figure 1) is suspended from the case with a spring. On impact, the magnetic field moves and the mass remains relatively still. This causes a relative motion between the coil (mass) and the transducer case (magnetic field). The voltage generated by this motion is proportional to the velocity of the coil relative to the transducer case. Depending on the frequency range, the velocity of the coil relative to the case may or may not be the actual velocity of the transducer case. When measurements are obtained at either the low or the high end of the transducer's frequency range, the output is usually not the actual velocity response of the transducer case. However, for a range of frequencies, the transducer response is directly

R. C. Graves, Kentucky Transportation Center, University of Kentucky, 533 South Limestone Street, Lexington, Ky. 40506. V. Drnevich, Department of Civil Engineering, University of Kentucky, 212 Anderson Hall, Lexington, Ky. 40506.

proportional to the actual velocity response of the transducer case, and it is independent of frequency. This concept is better shown in Figure 2, in which a velocity transducer output divided by actual velocity is plotted versus frequency. Between the points labeled A and B in Figure 2, the response of the transducer does not significantly change with frequency. However, below Point A and above Point B, the response of the transducer is frequency dependent.

Because the response of the pavement usually occurs in the frequency range 0 to 100 Hz, the frequency-dependent response function must be used to calculate the actual velocity from the given transducer output if accurate velocities are desired for the entire time history (*2,3*).

Transducer Simulation

To properly describe the velocity transducer as an SDOF system, the following characteristics must be known: undamped natural frequency, f_n, mass of the suspended body, m, and the damping ratio (fraction of critical damping, ξ). From these parameters, others, such as critical damping, spring constant, and undamped natural angular frequency, may be calculated (*5*).

A typical spring-mass system representing a velocity transducer is shown in Figure 3. The following displacements may
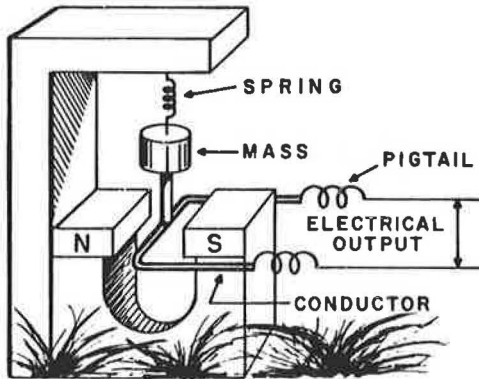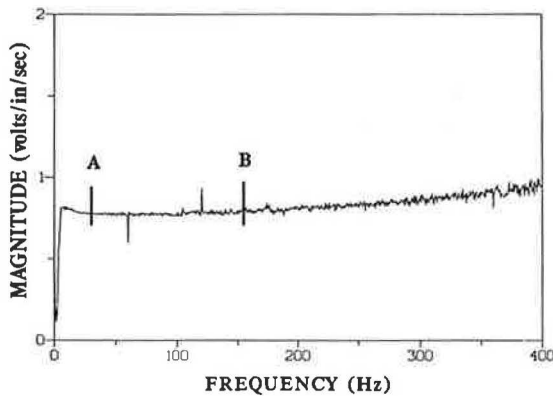

FIGURE 1   Typical transducer configuration (*4*).

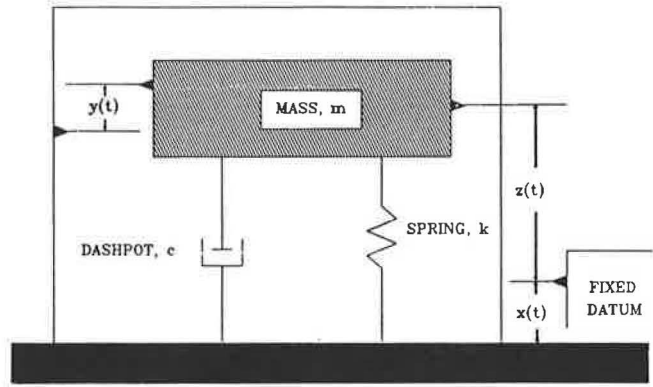**FIGURE 2   Typical transducer frequency response curve.**

FIGURE 3   Typical spring mass system.

be defined: $y(t)$ is the displacement between the mass and the transducer case; $x(t)$ is the displacement of the pavement (with attached transducer case) relative to a fixed datum; and $z(t)$ is the absolute displacement of the mass, defined as follows:

$$z(t) = x(t) + y(t) \tag{1}$$

If the pavement undergoes a movement $x(t)$, the response to the system may be derived from the equation of motion stating that the summation of forces in the vertical direction (including inertial forces) must equal zero. From a free-body diagram the following forces may be determined: the inertial force $m \cdot \ddot{z}(t)$, the spring force $k \cdot y(t)$, and the damping force $c \cdot \dot{y}(t)$. Summation of these forces yields the following:

$$m \cdot \ddot{z}(t) + c \cdot \dot{y}(t) + k \cdot y(t) = 0 \tag{2}$$

Substituting Equation 1 into Equation 2 and dividing both sides by the mass yields

$$\ddot{x}(t) + \ddot{y}(t) + \dot{y}(t)\frac{c}{m} + y(t)\frac{k}{m} = 0 \tag{3}$$

This equation may be solved for the pavement acceleration, $\ddot{x}(t)$, in terms of the acceleration, velocity, and displacement of the mass relative to the case.

$$\ddot{y}(t) + \dot{y}(t)\frac{c}{m} + y(t)\frac{k}{m} = -\ddot{x}(t) \tag{4}$$

Substitution of the known transducer characteristics of damping and natural frequency into Equation 4 gives

$$\ddot{y}(t) + \dot{y}(t)2\xi\omega_n + y(t)\omega_n^2 = -\ddot{x}(t) \tag{5}$$

where $\omega = 2\pi f_n$.

Equation 5 is the time domain representation of the SDOF system in Figure 3. Using Fourier analysis as presented by Ramirez (*6*), an equivalent equation of motion may be determined in the frequency domain. Taking the Fourier transform of both sides gives

$$\ddot{Y}(\omega) + \dot{Y}(\omega)2\xi\omega_n + Y(\omega)\omega_n^2 = -\ddot{X}(\omega) \tag{6}$$

where ω is the circular frequency ($2\pi f$) and $Y(\omega)$, $\dot{Y}(\omega)$, and

$\ddot{Y}(\omega)$ are the Fourier transforms of the displacement, velocity, and acceleration, respectively. Integration in the frequency domain is accomplished by multiplying the function by $(j\omega)^{-1}$, where $j = \sqrt{-1}$. Differentiation may be accomplished by multiplying the function by $j\omega$. Performing these operations leads to

$$\ddot{Y}(\omega) = -\omega^2 Y(\omega) \tag{7}$$

$$\dot{Y}(\omega) = j\omega Y(\omega) \tag{8}$$

and

$$\ddot{X}(\omega) = -\omega^2 X(\omega) \tag{9}$$

Substitution of these equations into Equation 6 yields

$$-\omega^2 Y(\omega) + 2\xi j\omega\omega_n Y(\omega) + Y(\omega)\omega_n^2 = -\omega^2 X(\omega) \tag{10}$$

Solving for $X(\omega)$ in terms of $Y(\omega)$ gives

$$X(\omega) = Y(\omega) \left(\frac{-\omega^2 + \omega_n^2 + 2\xi j\omega\omega_n}{-\omega^2} \right) \tag{11}$$

which, on rearrangement, becomes

$$X(\omega) = Y(\omega) \left[1 - \left(\frac{\omega_n^2}{\omega^2} \right) - \frac{2\xi j\omega\omega_n}{\omega^2} \right] \tag{12}$$

The inverse of the term in brackets in Equation 12 is called a transfer function of the transducer, because it is the system output divided by the system input. It is denoted by $H(\omega)$. Thus,

$$H(\omega) = \left[1 - \left(\frac{\omega_n^2}{\omega^2} \right) - \frac{2\xi j\omega\omega_n}{\omega^2} \right]^{-1} \tag{13}$$

Pavement Response Simulation

The pavement motion, which is the input to the velocity transducer, also may be simulated by using another equivalent SDOF model. As mentioned earlier, several system parameters must be defined to characterize the SDOF system. The parameters used for the velocity transducer and for the pavement are given in the following table.

Parameter	Velocity Transducer	Pavement
Natural frequency, f_n (Hz)	4.5	100
Damping ratio, ξ	0.6	0.4
Spring constant, k (lb/in.)	0.0867	1,000,000

Computer Simulation of the SDOF System

The solution to both SDOF models has been completed using the computer program DIRECT developed by Paz (7). The method of solution is exact for excitations that may be described by linear segments between points defining the excitation function. This is accomplished by linear interpolation between the data points. The response of each time interval is calculated by considering the initial conditions and a linear

excitation during the interval. The values calculated are the displacement, velocity, and acceleration time histories for the model given by the input parameters.

In this study, several types of forcing functions were applied to the pavement model (Figure 4). All the forcing functions have a duration of 0.025 sec and a maximum amplitude of 10,000 lb. Each forcing function, defined by 256 points, was entered into the computer program, and the resulting pavement displacement time histories were calculated.

In modeling the response of the velocity transducer on the pavement according to Equation 11, the acceleration of the pavement is used as the input excitation to the transducer. DIRECT was used again with the velocity transducer parameters and the pavement acceleration as input. A solution was determined for each of the forcing functions shown in Figure 4.

As indicated in Table 1, a change in shape of the forcing function changes the peak displacement response of the system, even when the duration and maximum input force are the same. This indicates that pavement deflection basins will vary somewhat from device to device for given peak force inputs. Although current convention (1,3) utilizes peak input force and peak displacements, better correlation among different devices could be obtained by using techniques such as root-mean-square (RMS) values (8) of both input force and measured displacement. In order to obtain RMS values of displacement, the entire time history must be accurately determined.

Pavement Displacement Determination from Velocity Transducer Model

A comparison of the pavement displacements from the pavement model with the integrated velocity transducer model outputs, which are the displacements of the mass relative to the transducer case, indicates that they are not the same. The results for the half-sine pulse are shown in Figure 5. The results for each forcing function are given in Table 1. Besides having different peak values, the integrated values are in error at all times and have peaks occurring at times different from the pavement model peak displacements.

Frequency Response Method for Displacement Calculations

The frequency response function given in Equation 13 is a true transfer function between pavement displacement and transducer displacement. It may be modified to calculate the pavement response (displacement) from the given transducer output.
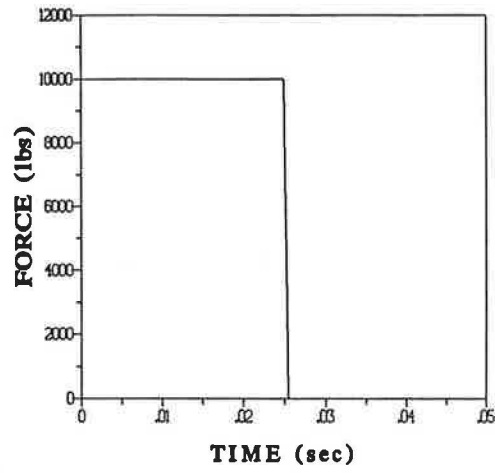
Solving Equation 12 for the pavement response in terms of the velocity transducer output gives the following:

$$X(\omega) = \dot{Y}(\omega) \left[\frac{1}{j\omega} - \left(\frac{\omega_n^2}{\omega^2 j\omega} \right) - \frac{2\xi\omega_n}{\omega^2} \right] \tag{14}$$
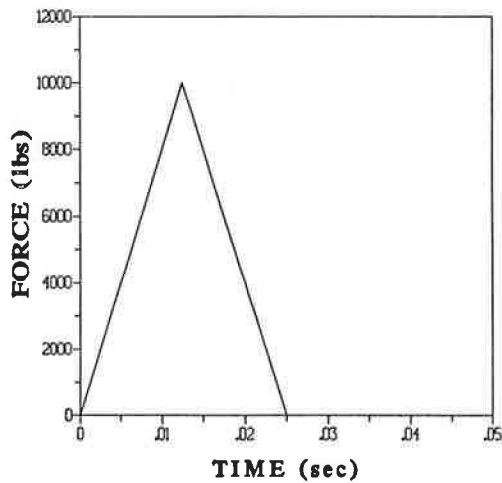
A transfer function, $H_v(\omega)$, may be defined as the ratio between the velocity transducer output $\dot{Y}(\omega)$ and the pavement displacement $X(\omega)$.
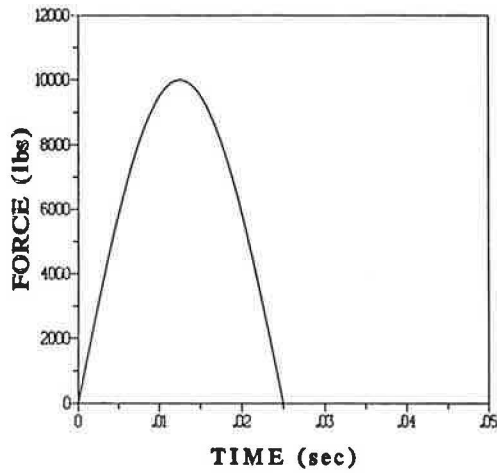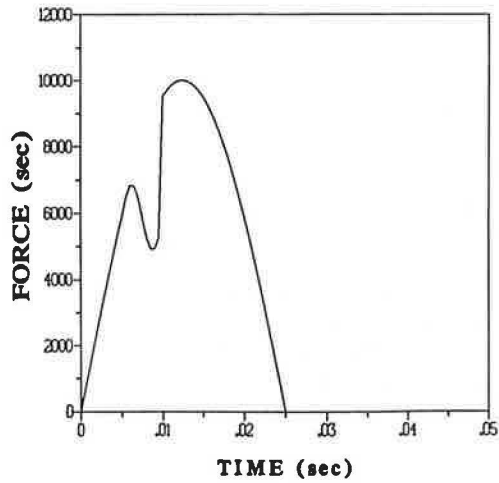
a. Half Sine Pulse

b. Square Pulse

c. Triangular Pulse

d. Glitch Pulse

FIGURE 4 Forcing functions.

TABLE 1   COMPARISONS OF PEAK DEFLECTIONS OF
PAVEMENT MODEL AND INTEGRATION OF VELOCITY
TRANSDUCER MODEL OUTPUT

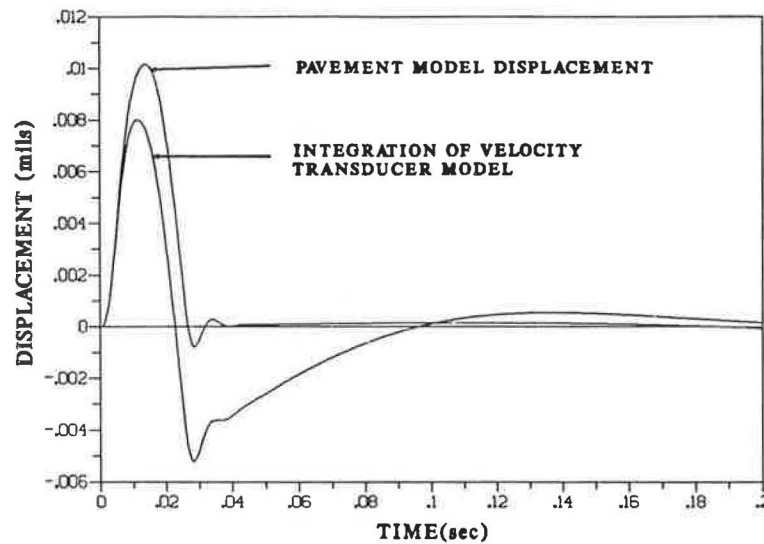| Type of Pulse	Deflection (mils)	
	Pavement	Transducer
Half Sine	10.22	7.98
Square	12.54	11.43
Triangle	9.93	7.75
Glitch	10.73	8.04

FIGURE 5 Displacement of pavement model and displacement calculated by integrating the transducer model output.

$$H_v(\omega) = \left[\frac{1}{j\omega} - \left(\frac{\omega_n^2}{\omega^2 j\omega} \right) - \frac{2\xi\omega_n}{\omega^2} \right]^{-1} \qquad (15)$$

By using Equation 14, the pavement displacement may be calculated from the output of the velocity transducer (i.e., the velocity of the transducer mass moving relative to the transducer case).

Calculation of the pavement displacement has been accomplished by programming Equation 14 in QuickBASIC and convoluting it with the transformed velocity transducer output. The velocity transducer output (relative velocity) is transformed to the frequency domain by using a Fast Fourier Transform (FFT) (6). After conversion to the frequency domain, the velocity is convoluted with the frequency response function $H(\omega)$ defined in Equation 15 by using complex multiplication. The pavement displacement versus time is then calculated using the inverse FFT. The maximum calculated displacements from the velocity transducer outputs and the displacements of the pavement model are compared in Table 2. There is excellent agreement between the two.

PHASE 2: LABORATORY CALIBRATION OF VELOCITY TRANSDUCERS

Background

The objective of calibrating velocity transducers is to determine their sensitivity, defined as the ratio of the electrical output to mechanical input applied to the specified axis (9). The relationship between the transducer sensitivity and frequency is commonly referred to as the calibration curve, transfer function, or frequency response function of the transducer. A typical one is shown in Figure 2.

Because the responses created by the FWD are transient, they contain frequency components that are predominantly in the range 0 to 100 Hz. The response of a typical velocity

TABLE 2 COMPARISON OF ACTUAL PAVEMENT MODEL AND TRANSDUCER-CALCULATED OUTPUT DISPLACEMENT USING FREQUENCY RESPONSE METHOD

Type of Pulse	Deflection (mils)	
	Actual	Calculated
Half Sine	10.22	10.22
Square	12.54	12.52
Triangle	9.93	9.87
Glitch	10.73	10.67

transducer is not linear throughout this range (see Figure 2). Therefore, for the analysis of these responses, the frequency response of the transducer must be established over this frequency bandwidth.

The theoretical representation of a transducer modeled as an SDOF system was developed in Equation 12. However, most velocity transducers do not behave as theory predicts; empirically developed frequency response functions are necessary to characterize them.

The fastest and most economical form of transducer calibration is the comparison method. This method involves simultaneous measurement of the outputs of the device under test and some reference device of known and stable conditions, with both devices subjected to the same excitation (9).

Most calibrations are conducted using an electrodynamic shaker that can produce various excitations depending on the voltage applied to its armature. The reference device is normally an accelerometer or a velocity transducer built into the shaker system. The frequency response function for this system may be defined as

$$H(f) = \frac{S_y}{S_x} \cdot \frac{S_x^*}{S_x^*} = \frac{G_{yx}}{G_{xx}} \qquad (16)$$

where

S_y = linear Fourier spectrum of the output,
S_x = linear Fourier spectrum of the input,
S_x^* = complex conjugate of S_x,
G_{yx} = cross power spectrum, and
G_{xx} = auto power spectrum.

A velocity transducer can be considered to be a linear system up to limits defined by the travel of its coil. This means that the response of the transducer is proportional to its excitation (9). Because the transducer is considered a linear system, its response is independent of the excitation magnitude to which it is subjected (10). Therefore, any type of excitation of the shaker—swept-sine, random noise, or impulse—could be used to calibrate the transducer.

Frequency Response Curves for FWD Velocity Transducers

Calibration System

A velocity transducer of the type used in FWDs was mounted on an electrodynamic shaker that had an internal velocity transducer. An audio range oscillator was used to supply a single ramp function having a rise time of 24 msec to the shaker. The velocity of the shaker armature and the output of the FWD-type transducer were simultaneously recorded by the analyzer, a Hewlett Packard 3562A Dynamic Signal Analyzer. The use of the shaker velocity transducer to determine armature displacement was validated by attaching a displacement transducer, an LVDT, to the shaker armature and comparing the two. Excellent agreement was obtained to frequencies of 20 Hz, where the LVDT data became erratic because of vibration of the LVDT support system (2). For higher frequencies, a seismic accelerometer with linear range from 0.07 Hz to 800 Hz was used. It also provided excellent agreement. Details are given elsewhere (2).

The resulting displacement history of the shaker armature is shown as one of the curves in Figure 6. The shape of this curve is similar to that of the theoretical curve developed in Phase 1 and given in Figure 5.

Time Domain Integration of Data of the FWD-Type Transducer

Because the net displacement after applying the ramp function was zero, the output of the FWD-type transducer was corrected to zero by subtracting (or adding) the corresponding average values from (or to) all 2,048 data points. The signal was then converted to displacement by simple, time-domain integration. The resulting integrated time history displayed a very small negative value at time zero even though no displacement existed. This small value was added to all integrated values (i.e., the zero axis was shifted downward a small amount).

The resulting curve for the time-domain-integrated, FWD-type velocity transducer is also shown in Figure 6. It is clearly different from that of the shaker armature, which is the displacement applied to the transducer case. It differs not only in magnitude but also in times to the peak values. This is expected according to the theory for velocity transducers as discussed in Phase 1 and shown in Figure 5.

Generation of the Frequency Response Function for the FWD-Type Transducer

The frequency response function for the FWD-type velocity transducer was obtained directly by using the analyzer's frequency response function, which operates according to Equation 16. This is equivalent to transforming both curves shown in Figure 6 using the FFT function and then, in the frequency domain, dividing the FWD-type transducer curve by the curve for the actual displacement. The resulting curve is the frequency response function for the FWD-type transducer, which is shown in Figure 7. The curve is well defined at low frequencies but is not well defined at frequencies above 100 Hz.
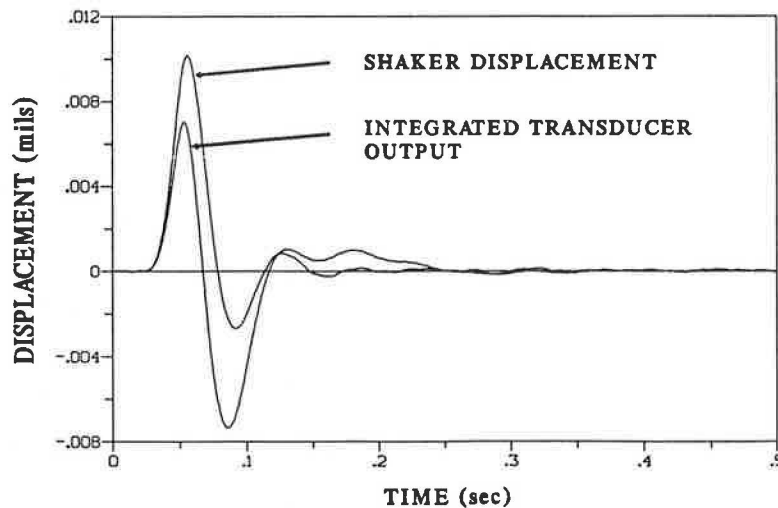

FIGURE 6   Actual displacement of the transducer case and displacement of transducer mass relative to the transducer case.
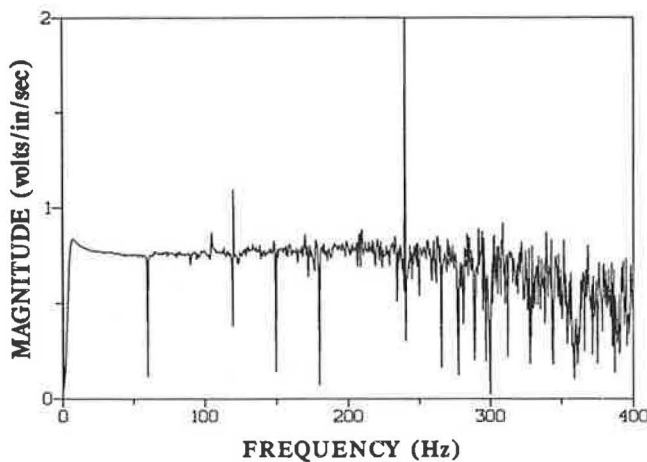
FIGURE 7   Frequency response function calculated using the ramp excitation.

The reason is that the displacement applied to the transducer was deficient in high-frequency components.

Hybrid Frequency Response Function for the FWD-Type Transducer

According to the theory discussed earlier, the frequency response function should be independent of the type of excitation. The FWD-type transducer was calibrated a second time with the excitation being random noise having a 0- to 400-Hz bandwidth. (The analyzer has a built-in random noise generator.) The same process was applied to these outputs as was applied to the one with the ramp excitation. The resulting curve is given in Figure 2. Comparison of the two indicates that they are similar in shape and magnitude. Closer examination reveals that the ramp-generated curve has more consistent values at frequencies less than 25 to 50 Hz, the random-noise-generated curve has more consistent values in frequencies above this range, and values in the 25- to 50-Hz range are practically identical. The two responses were combined to form a hybrid frequency response curve, as shown in Figure 8. The two response functions were combined at a
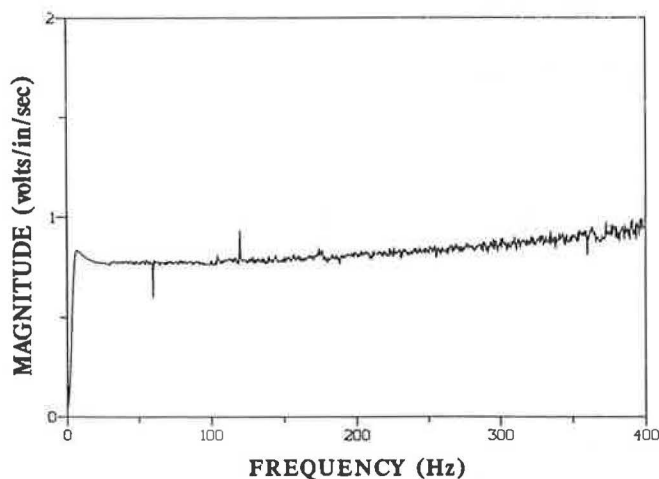
FIGURE 8   Hybrid frequency response function.

specified frequency in the 25- to 50-Hz range to obtain a frequency response function that is accurate across the complete frequency bandwidth.

Checking the Hybrid Frequency Response Function

To check its accuracy, the hybrid frequency response function was used on the FWD-type transducer output to obtain a calculated displacement. The process involved the following steps:

1. Transform the transducer voltage output from the time domain to the frequency domain by use of the FFT.
2. Divide the transformed data by the FWD-type frequency response function.
3. Integrate the signal to obtain frequency domain values proportional to the displacement of the transducer case.
4. Inverse transform the result back to the time domain.
5. Check the initial displacement. It should be zero. If it is not, adjust all displacement values by the appropriate amount to obtain zero initial conditions.

The resulting displacement is plotted in Figure 9 along with the displacement determined by the shaker transducer. The two curves are not distinguishable. By use of the analyzer, it was established that the peak values differed by less than 1 percent and that the average difference in displacement over the time range 0 to 200 msec was less than 0.1 mil.

Behavior for Another Frequency Bandwidth

All of the above procedures were repeated for a frequency bandwidth of 0 to 100 Hz (which corresponds to the 8-sec data acquisition time). Similar results were obtained, and the differences between the measured and calculated displacements were even smaller (e.g., peak difference less than 0.25 percent). The improved accuracy was due to a combination of displacement time history curve smoothing caused by the longer interval between data points (4 msec versus 1 msec) and the increased accuracy of the frequency response function caused by more closely spaced frequency lines (0.125 Hz versus 0.5 Hz). The technical term for the latter phenomenon is reduced leakage (6), which is discussed subsequently.

In the frequency domain, data can only be determined at the frequency lines that are spaced Δf apart. Components with frequencies between the frequency lines are "leaked" to adjacent frequency line values. For the cases studied, very low frequency components between the first frequency line at 0 Hz and the second frequency line at $0 + \Delta f$ Hz are leaked to the 0 Hz and the Δf Hz lines. On performing the inverse transform to obtain the time domain data, the 0 Hz component registers as a DC offset.

Another possible cause of the DC offset is the periodicity of the input that is inherently assumed in Fourier transformations. Veletsos and Ventura described this phenomenon in detail (11). The assumption is that the time record repeats itself indefinitely (i.e., at the end of the time record, exactly the same signal recurs). Real FWD signals are transient and last less than 0.5 sec. The entire time record for a 400-Hz
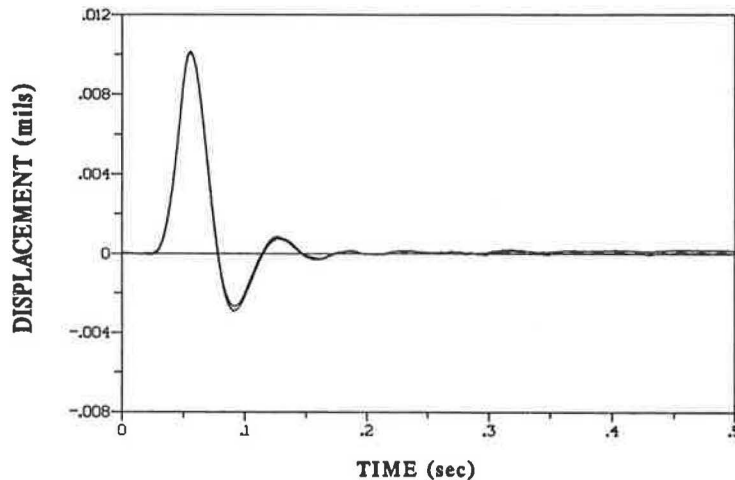
FIGURE 9   Comparison of shaker displacement and FWD-type transducer calculated displacement.

bandwidth is 2 sec. Hence, a "quiet time" that lasts 1.5 sec or longer follows the FWD signal. This problem is identified by values of both DC offset and nonzero slope at time zero on the inverse transformed signal. Close examination of the inverse transformed signals showed the DC offset but zero slope, and it was concluded that the DC offset was not caused by this phenomenon. The fact that vertically loaded pavements exhibit high damping also supports this conclusion.

PHASE 3: COMPARISON OF DEFLECTIONS WITH THOSE FROM AN FWD DEVICE

FWD Apparatus and Location of Verification Site

The FWD used in this study was a JILS-20, manufactured by Foundation Mechanics, El Segundo, California. The test location, referred to as the garage, was in the garage adjacent to the research building. The pavement structure there consisted of 6 in. of portland cement concrete over 4 in. of crushed stone over a compacted subgrade. Bedrock is located approximately 10 ft below the surface.

Comparison Setup

Two FWD-type velocity transducers, which were calibrated during Phase 2, were used for this testing and were independent of those used as sensors on the FWD. The comparison process, similar to the process used by Nazarian and Bush (*3*), consisted of rigidly attaching the independent, FWD-type transducers to the pavement as close to the actual FWD sensors as possible. The FWD sensors were located at distances of 0, 1, 2, 3, 4, 5, and 6 ft and were labeled Locations 1 through 7. To ensure that the independent transducers remained securely attached in this location, they were screwed to aluminum disks that were glued to the pavement. The FWD sensors were held in place by springs attached to the sensor boom. For the displacement comparison, one transducer was used as a reference and remained at Location 2 while the

other was moved to Locations 3 through 7. It was not possible to place a transducer adjacent to the transducer at Location 1 because of the loading plate surrounding it.

The recording device was a Hewlett Packard 3562A Dynamic Signal Analyzer. Because it is a two-channel analyzer, a new set of data must be obtained as the transducer is moved to each new position. The output from the reference transducer is connected to Channel 1 while the output of the other transducer is connected to Channel 2. All data were taken over a 2-sec time record, as in Phase 2.

Test Procedure

Both single- and multiple-drop tests were performed. The JILS-20 FWD can take up to four successive measurements at a given location before the boom and loading plate are raised from the pavement. Because the analyzer can average the measurements, tests were conducted using both a single drop and a four-drop series. For the four-drop tests, the voltage time histories taken by the analyzer were averaged using time domain averaging. The displacement was then calculated from the averaged velocity signal. For the FWD data, four peak displacements were calculated by the FWD software. The four peak displacements were averaged and then compared with the average displacement calculated by the analyzer. This test procedure was carried out at the site for loads of 7,000 and 14,000 lb.

Displacement Determination

Calculation of the displacements using the analyzer with signals from the independent transducers was done in the same manner as for Phase 2. Typical results for each step are given below for one sensor location with a 7,000-lb load with a single drop.

The raw voltage output of the independent transducer at Location 4 (3 ft from the center of the load) is shown in Figure 10. This signal, transformed to the frequency domain, is given
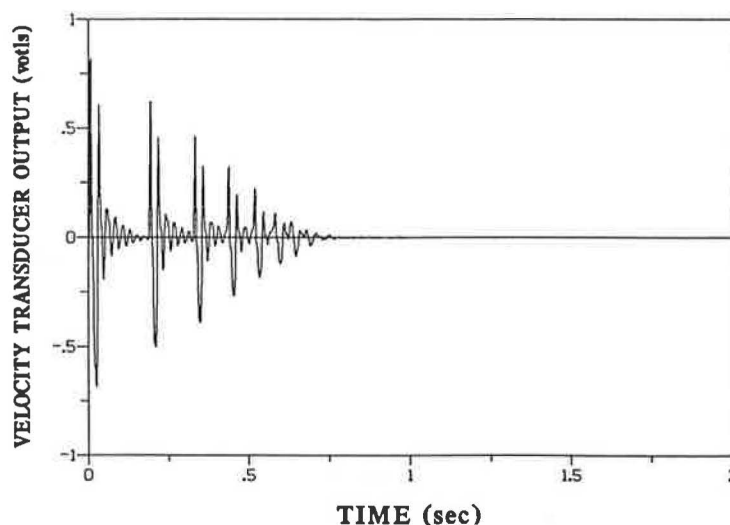
FIGURE 10 Raw velocity output of independently calibrated transducer at Location 4.

in Figure 11. Integration in the frequency domain is carried out by multiplying by $j\omega^{-1}$, and convolution is accomplished by dividing the integrated signal by the frequency response function for that transducer. The result is the pavement displacement in the frequency domain shown in Figure 12. An inverse transform is then performed to obtain the pavement displacement in the time domain, that is, the pavement displacement time history. The time history is then corrected for DC offset. The final pavement displacement is given in Figure 13.

Examination of the displacement in Figure 13 indicates some interesting features. First, multiple hits have occurred, and multiple displacement responses are observed. They are identified as such because each subsequent response has diminished amplitude and occurs at a shorter interval. (Bedrock reflections would occur at constant intervals.) The traces also indicate that motion at the sensor consists of multiple cycles of vibration that are highly damped. Because the entire time history should be accurate, these characteristics present some powerful possibilities, such as determining pavement response to multiple force levels from a single test and obtaining pavement damping characteristics.

Displacement Comparisons

FWD deflections are used to determine deflection basins for each location. The deflection basin is a plot of maximum displacement versus radial distance from the center of the load. Deflections at each sensor location for a single test and for a four-test average are included in Figures 14 and 15, respectively. Both the FWD-calculated and the analyzer-calculated deflections are shown.

The difference in the deflections for each basin is calculated as the difference between the analyzer- and FWD-calculated deflections. The differences are shown as the percentage of
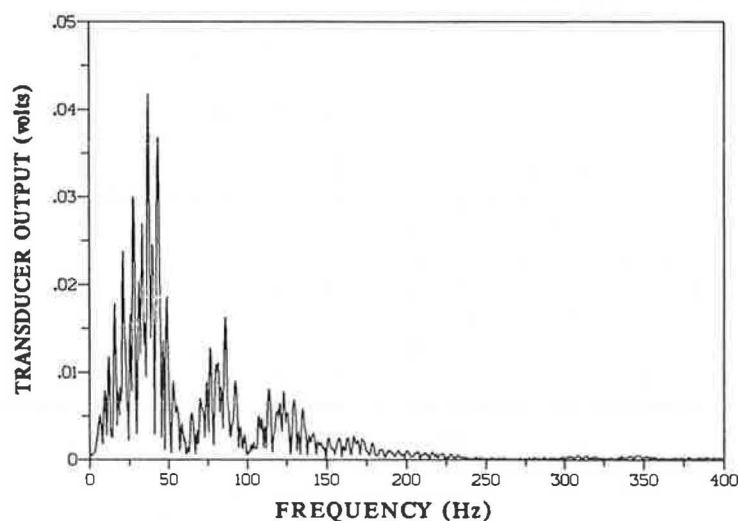
FIGURE 11 Frequency domain representation of transducer output.
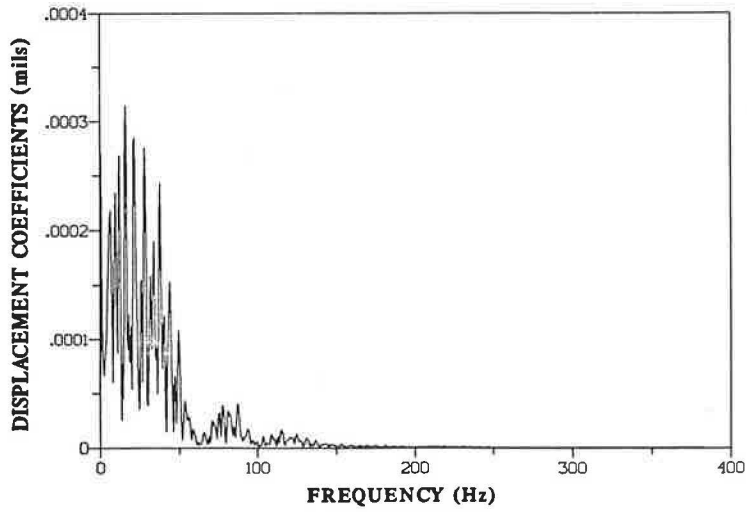
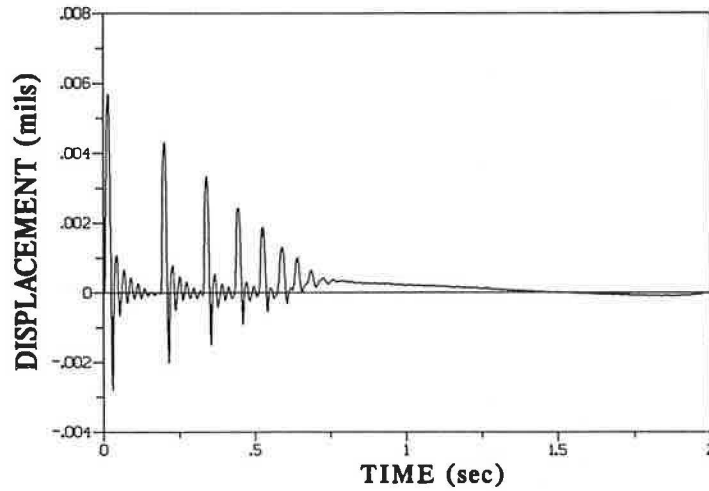FIGURE 12   Frequency domain representation of calculated displacement.

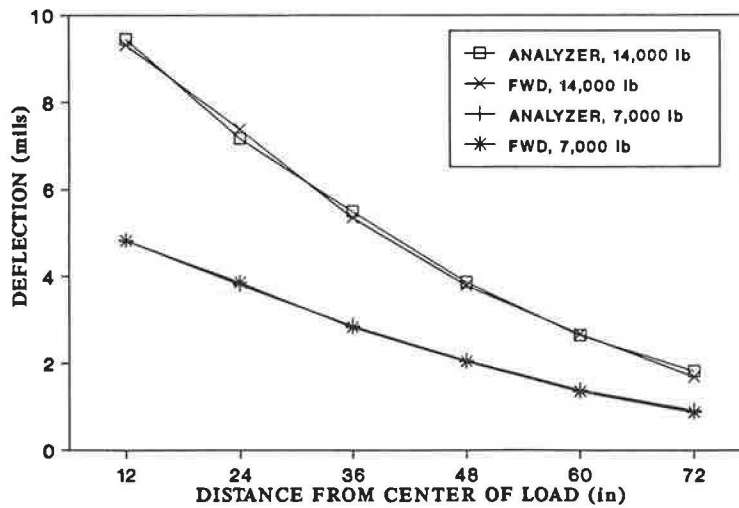FIGURE 13   Calculated deflection time history of pavement.

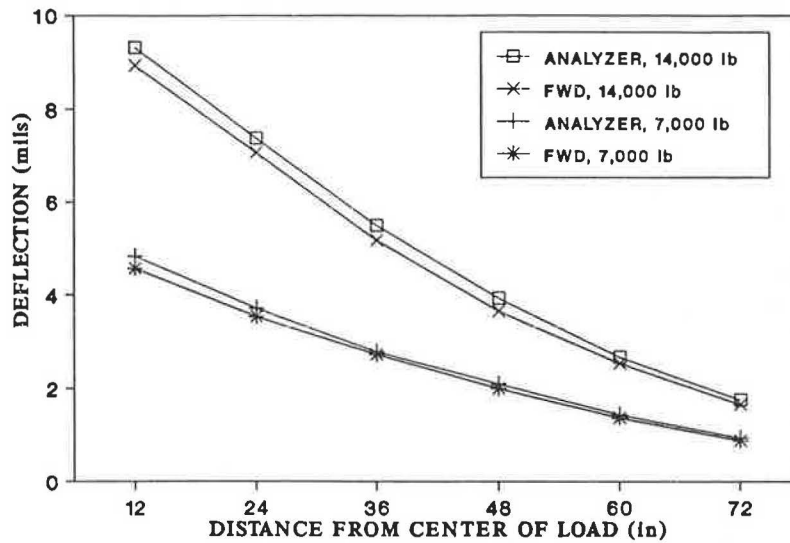FIGURE 14   Deflection basin, garage floor, single test, 7,000 and 14,000 lb.

FIGURE 15 Deflection basin, garage floor, four-test average, 7,000 and 14,000 lb.

the maximum analyzer-calculated deflection. Tables 3 and 4 summarize the results for the single drop tests at two different loads, and Tables 5 and 6 summarize the results for the multiple-drop tests. For perspective, other studies have noted that the precision of measurements with an FWD is generally within ±5 percent (3).

Discussion of Differences

Tables 3 through 6 indicate that, for the garage floor, the difference between the deflections determined by the two methods is greater for the four-test average than for the single-drop tests. The differences obtained from the single tests are generally between −3 and +7 percent, and the differences from the four-test average are between +2 and +8 percent. The deflections determined by the independent transducers tend to be larger than those determined by the JILS-20 FWD transducers and software. The reason for this is not known and is being studied. Some of the differences between the two types of tests may be attributed to the method of aver-

aging. The analyzer averages the raw velocity trace before it is used to calculate the displacement. The average values of the FWD displacements are calculated from the average of the four individual peak displacements.

TABLE 4   DEFLECTION COMPARISON, 14,000 lb, GARAGE FLOOR, SINGLE TEST

Sensor Location	Displacements (mils)		Percent Diff.
	FWD	Analyer	
3	7.39	7.18	-2.92
2	9.36	9.34	-0.21
4	5.36	5.50	2.54
2	9.46	9.47	0.10
5	3.79	3.87	2.07
2	9.32	9.45	1.37
6	2.68	2.65	1.12
2	9.54	9.52	0.21
7	1.69	1.82	7.14
2	9.57	9.58	0.10

TABLE 3   DEFLECTION COMPARISON, 7,000 lb, GARAGE FLOOR, SINGLE TEST

Sensor Location	Displacements (mils)		Percent Diff.
	FWD	Analyzer	
3	3.87	3.82	-1.31
2	4.92	4.96	0.81
4	2.84	2.87	1.05
2	4.94	4.90	-0.81
5	2.04	2.06	0.97
2	4.82	4.84	0.41
6	1.36	1.39	2.16
2	4.78	4.84	1.24
7	0.87	0.92	5.43
2	4.81	4.87	1.23

TABLE 5   DEFLECTION COMPARISON, 7,000 lb, GARAGE FLOOR, FOUR-TEST AVERAGE

Sensor Location	Displacements (mils)		Percent Diff.
	FWD	Analyzer	
3	3.54	3.72	4.84
2	4.45	4.72	5.72
4	2.72	2.78	2.16
2	4.57	4.85	5.77
5	2.00	2.10	4.76
2	4.62	4.86	4.94
6	1.37	1.43	4.19
2	4.57	4.83	5.38
7	0.88	0.94	6.38
2	4.60	4.87	5.54

TABLE 6   DEFLECTION COMPARISON, 14,000 lb,
GARAGE FLOOR, FOUR-TEST AVERAGE

Sensor Location	Displacements (mils)		Percent Diff.
	FWD	Analyzer	
3	7.07	7.38	4.20
2	9.03	9.48	4.75
4	5.17	5.49	5.82
2	8.93	9.32	4.18
5	3.65	3.92	6.89
2	8.86	9.23	4.01
6	2.54	2.67	4.87
2	8.75	9.16	4.47
7	1.66	1.76	5.68
2	8.97	9.36	4.17

The FWD software uses a single frequency response function for all seven velocity transducers, whereas the individual frequency response functions were used with the independent transducers. Variations among transducers could account for some of the observed differences, especially the variation from one transducer location to another.

As discussed in Phase 2, displacements determined by use of frequency response functions are sensitive to values of the frequency response functions at very low frequencies. Some of the consistent differences could be due to small differences in the frequency response functions at the low frequencies. A comparison of a typical field deflection calculated by the different frequency response curves is presented in Table 7 for the 7,000-lb load. Table 7 indicates that the difference in frequency response function may affect the calculated displacement.

SUMMARY AND CONCLUSIONS

The frequency response function method is a feasible approach to accurately calculating displacement time histories from measurements made with velocity transducers. This was verified by use of classical mathematical models to describe pavement and transducer behavior. The models also were used to demonstrate that the shape of the loading function influences the peak displacement even when the peak load and duration of loading are kept constant. The procedures were validated in the laboratory utilizing an electrodynamic shaker and an FWD-type velocity transducer. It was found that the accuracy of the method depends on obtaining accurate frequency response functions, especially in the very-low-

TABLE 7   FREQUENCY RESPONSE FUNCTION EFFECTS
ON ACTUAL FIELD DEFLECTIONS, 7,000-lb LOAD,
SINGLE TEST

Frequency Response Function	Displacement (mils)	Percent Diff. from FWD
Random Noise	5.42	1.10
Impulse	5.54	3.25
Hybrid	5.50	2.54
FWD	5.36	0.00

frequency range, where the function varies greatly with frequency.

A comparison was made at one site with independent transducers used side by side with those of a JILS-20 FWD. Agreement between the two was generally good, but deflections determined by use of the independent transducers gave slightly larger deflections, on the average, than those from the FWD sensors and software. Reasons for these differences include methods of averaging and accuracy of the frequency response functions for specific transducers, especially in the low-frequency range.

The frequency response function approach gives accurate time histories for the entire time record. This is important because it allows for determining accurate deflection basins that account for different shapes of loading functions. It also may allow for calculating pavement response to multiple force levels from a single test, because data associated with the bounces could be used. This could mean a savings in both testing time and expense.

REFERENCES

1. M. S. Hoffman and M. R. Thompson. Comparative Study of Selected Nondestructive Testing Devices. In *Transportation Research Record 852*, TRB, National Research Council, Washington, D.C., 1983, pp. 32–40.
2. R. C. Graves. *Pavement Deflection Determination Using Velocity Transducers*. Master's thesis. University of Kentucky, Lexington, 1989.
3. S. Nazarian and A. J. Bush III. Determination of Deflection of Pavement Systems Using Velocity Transducers. In *Transportation Research Record 1227*, TRB, National Research Council, Washington, D.C., 1989, pp. 147–158.
4. *Mark Products Catalog*. Mark Products, Inc., Houston, Tex., 1989.
5. M. Paz. *Structural Dynamics Theory and Computation*. Van Nostrand Reinhold, New York, 1980.
6. R. W. Ramirez. *The FFT Fundamentals and Concepts*. Prentice-Hall, Inc., Englewood Cliffs, N.J., 1985.
7. M. Paz. *Microcomputer-Aided Engineering Structural Dynamics*. Van Nostrand Reinhold, New York, 1986.
8. V. P. Drnevich. Operating Characteristics of the WES 16-Kip Vibrator for the Nondestructive Testing of Pavements. *University of Kentucky Soil Mechanics Series*, No. 32, May 1985.
9. C. M. Harris. *Shock and Vibration Handbook* (3rd ed.). McGraw-Hill, New York, 1988.
10. *Application Note 243: The Fundamentals of Signal Analyses*. Hewlett Packard Company, 1985.
11. A. S. Veletsos and C. E. Ventura. Pitfalls and Improvements of DFT Method of Dynamic Analysis. *Structural Research at Rice*, Report 28, Department of Civil Engineering, Rice University, Houston, Tex., Aug. 1984, 37 pp.